An Adaptive Oscillators-Based Approach to Achieve Transparent Control of a Six DoF Lower-Limb Exoskeleton

(Article begins on next page)

An Adaptive Oscillators-Based Approach to Achieve Transparent Control of a Six DoF Lower-Limb Exoskeleton

Rafhael Milanezi de Andrade
Graduate Program of Mechanical Engineering
Universidade Federal do Espírito Santo
Vitória, ES, Brazil
rafhael.andrade@ufes.br ORCID: 0000-0002-2839-3649

Benito Lorenzo Pugliese
Department of Electronics and Telecommunication
Politecnico di Torino,
Turin, Italy
bpugliese@mgb.org

Abolfazl Mohebbi
Department of Mechanical Engineering
Polytechnique Montreal
Montreal, Canada
abolfazl.mohebbi@polymtl.ca

Paolo Bonato
Department of Physical Medicine & Rehabilitation
Harvard Medical School, Spaulding Rehabilitation Hospital
Boston, MA, USA
pbonato@mgh.harvard.edu

***Abstract*— Lower-limb exoskeletons have been effectively used in rehabilitation to reduce gait impairments. However, making the exoskeleton transparent to provide suitable net interaction torques and assist patient's movements is yet an open challenge. In this study, we designed a torque control method based on adaptive oscillators (AOs) to reduce interaction forces with a six degree-of-freedom exoskeleton, named the ExoRoboWalker. A synchronization layer was designed with a pool of AOs to estimate user's gait phase, and a baseline torque controller was introduced to generate a torque profile based on user-robot interaction during the previous gait cycles. A zero-torque controller was used in parallel to the main torque controller with the objective of improving users' control of the system and their balance. The proposed controller was experimentally evaluated in eight healthy subjects who walked with the exoskeleton for 200 gait strides at different walking speeds. A transparent controller we previously implemented based on a zero-impedance model was also evaluated and results were compared with the new controller. The controller based on AOs was able to reduce the average interaction torques by 40% at the highest gait speed of 0.8 m/s relative to the zero-impedance controller we previously implemented.**

Keywords—Adaptive Oscillators, Human-Robot Interaction, Lower-Limb Exoskeleton, Transparent Controller.

I. Introduction

Lower-limb exoskeletons (LLE) have been successfully used for gait rehabilitation over the last two decades [1]. Several designs for LLE actuators, links, degrees of freedom (DoF), and control systems have been proposed to improve clinical outcomes by achieving a target lower limb kinematics and kinetics [2]. LLE can be divided into three main categories: overground walking exoskeletons [3], treadmill-based exoskeletons [4], and walker-linked exoskeletons [5]. While in treadmill-based and walker-linked exoskeletons the weight of the system is transferred to the base structure, in overground walking exoskeletons the weight of the system is borne by the user [6].

Unlike position-based control approaches, where the output position of the LLE is set irrespective of the physical interaction with the user [2], in modern LLE control systems based on the assistance as needed concept [7], relying on impedance or admittance control [8], the torques transferred to the user should properly cancel the dynamic effects of structural weight, inertia, and friction [9]. Hence, the system should not interact with the user if no assistance is necessary, i.e., the exoskeleton should be transparent to the user. The transparency of the system is even more important in overground walking exoskeletons, where the user controls the motion [10].

Previous transparent controller systems sought to estimate user-robot interaction and compensate for it using different methodologies. Zanotto et al. [11] proposed a zero-torque controller using an integrated loadcell in the ALEX II treadmill-based exoskeleton's supporting cuffs. Mendonza-Crespo et al [9] designed a transparent controller based on gravity, friction, and interaction force compensation. Andrade et al [12] introduced a feedback zero-torque controller with feedforward compensation for dynamic effects and actuators' impedance in the ExoRoboWalker, a six DoF overground walking LLE. Küçüktabak et al. [13] introduced a whole-exoskeleton close-loop compensation transparent controller based on estimated interaction torques, measured joint torques, and a constrained optimization method integrated with a virtual model controller to track desired interaction torques in a closed loop. Camardella et al [14] proposed a transparent control algorithm that continuously blends the output of two independent single stance dynamic models based on the gait phase. Still, interaction forces between the user and the exoskeleton are larger than it would be clinically desirable, thus limiting clinical adoption of this technology.

Controllers based on adaptive oscillators (AOs) provide an interesting alternative to traditional approaches. AOs are nonlinear oscillatory dynamic systems capable of synchronizing their phase and frequency in response to an external input [15]. AOs have been recently used to estimate the gait phase and deliver motion assistance via assistive lower-limb devices to achieve changes in gait patterns [16][17]. In this paper, we introduce an innovative transparent controller designed using AOs to improve transparency of the ExoRoboWalker [12]. The method is generally applicable to cyclical movements and herein tested during walking. A pool of AOs is utilized to synchronize with the LLE cyclical movements and estimate the gait phase as well as the start time of each stride. A baseline torque controller is used to generate a continuous output torque for the entire gait cycle based on the physical user-robot interaction during the previous gait cycles. A zero-torque controller is utilized in parallel to the main transparent controller to allow for better volitional control by the user.

II. Methodology

A. The ExoRoboWalker

The ExoRoboWalker, Fig. 1, is a six DoF overground walking LLE designed to guide hip, knee, and ankle movements of both legs in the sagittal plane. The exoskeleton's mechanics comprises six harmonic drive-based actuators composed by an EC 45 flat 70W brushless motor (Maxon Motors, Switzerland) and a CSD-20-2a harmonic drive, with gear ratio of 160 (Harmonic Drive LLC, USA). Aluminum made lateral bars link the actuators to the lumbar support, insoles, and cuffs. A potentiometer is embedded in each actuator to measure joint angles. User-robot interaction torques are measured by strain gauges arranged in a full Wheatstone bridge hence measuring torque at each joint. Two force sensing resistors are integrated in insoles to detect the gait phase. Data is transferred from the sensors to the control hardware via a CAN BUS. The core of the control architecture is a Speedgoat Baseline real-time target computer (Speedgoat, MA, USA) with a 2 GHz quad-core CPU that runs a Matlab kernel. The control algorithms are implemented in Simulink using the Real-Time toolbox.

B. AO-Based Transparent Controller

The proposed torque controller, presented in Fig. 2, is designed to improve transparency of the ExoRoboWalker during cyclical movements such as walking, and consists of a high-level controller that runs on the Speedgoat Baseline real-time target computer (Speedgoat, MA, USA) using Simulink Matlab (Mathworks, MA, USA) and a low-level torque controller implemented using the motor drivers (AZBH12A8, Advanced Motion Controls, CA, USA). The baseline torque controller is the core of the high-level controller and generates a torque profile based on the joint torques recorded during the previous strides to reduce the human-robot interaction forces during the next gait cycle.

The synchronization layer uses a pool of AOs, that are dynamic systems able to adapt to cyclical movements [15][17], and to enable gait event detection, phase correction and stride counting to synchronize with the movements of the user with the control of the robot. Moreover, to allow for volitional control of the exoskeleton by the user, a baseline torque controller runs in parallel to a zero-torque controller.

1) Synchronization layer

Adaptive oscillators are used to estimate the difference between right and left hip angle ($\hat{\theta}_{RL}$) as a sum of sinusoidal functions as follows:

$$\hat{\theta}_{RL}(t) = \alpha_0(t) \sum_{n=1}^{3} \alpha_n(t) \sin\big(\varphi_n(t)\big) \tag{1}$$

where $\alpha_n(t)$ is the amplitude, $\varphi_n(t)$ is the phase and $\alpha_0(t)$ is the offset used to reconstruct the input signal $\theta_{RL}(t) = \theta_{RightHip}(t) - \theta_{LeftHip}(t)$. The number of harmonics was set to three as suggested by [16][17].

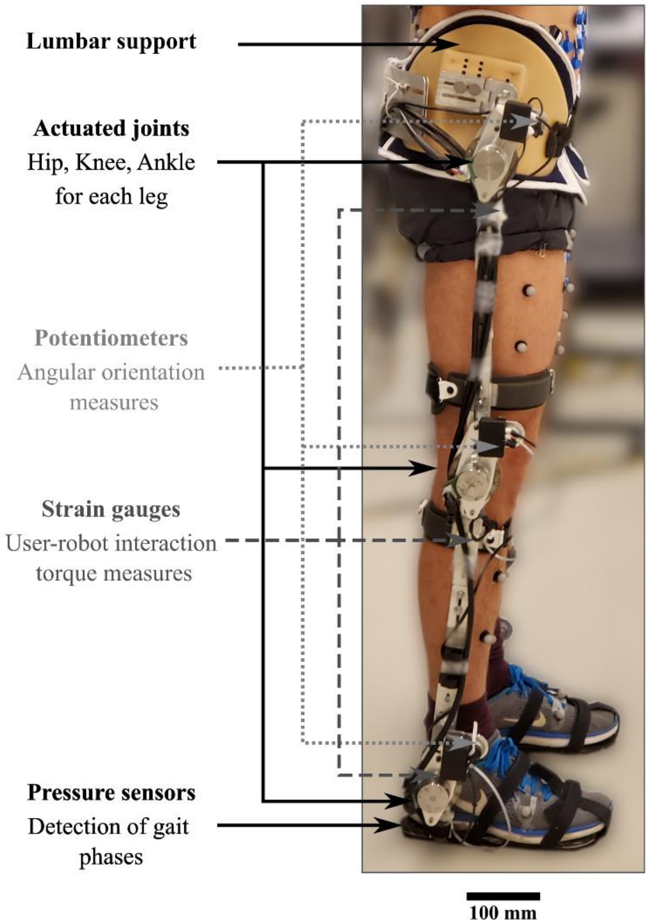

Fig. 1. The ExoRoboWalker is composed by six harmonic drive-based actuators assembled on the hip, knee and ankle joints, lateral bars between actuators, lumbar support, and insoles. The sensing comprises custom torque sensors to measure user-robot interaction, one potentiometer in each joint, and two force sensing resistors on each insole.

The states in Eq. (1) were obtained using the following equations:

$$\dot{\varphi}_n(t) = \omega(t)n + \nu_\varphi \frac{F(t)}{\sum \alpha_n} \cos\big(\varphi_n(t)\big) \tag{2}$$

$$\dot{\omega}(t) = \nu_\omega \frac{F(t)}{\sum \alpha_n} \cos\big(\varphi_1(t)\big) \tag{3}$$

$$\dot{\alpha}_n(t) = \eta\, F(t) \sin\big(\varphi_n(t)\big) \tag{4}$$

$$\dot{\alpha}_0(t) = \eta\, F(t) \tag{5}$$

where $F(t) = \theta_{RL}(t) - \hat{\theta}_{RL}(t)$ is the angle estimation error which drives the convergence of the dynamic system, and $\omega(t)$ is the fundamental frequency of the system. The gains $\nu_\varphi = 4$, $\nu_\omega = 4$ and $\eta = 1$ determine the learning speed of the phase, frequency, and amplitude, respectively. They were heuristically tuned to provide fast and stable adaptation.

The fundamental phase ($\varphi_1(t)$) of the system is normalized to be in the range [0, 2π] to obtain the gait phase of the exoskeleton $\varphi_{GP}(t)$:

$$\varphi_{GP}(t) = mod(\varphi_1(t), 2\pi) \tag{6}$$

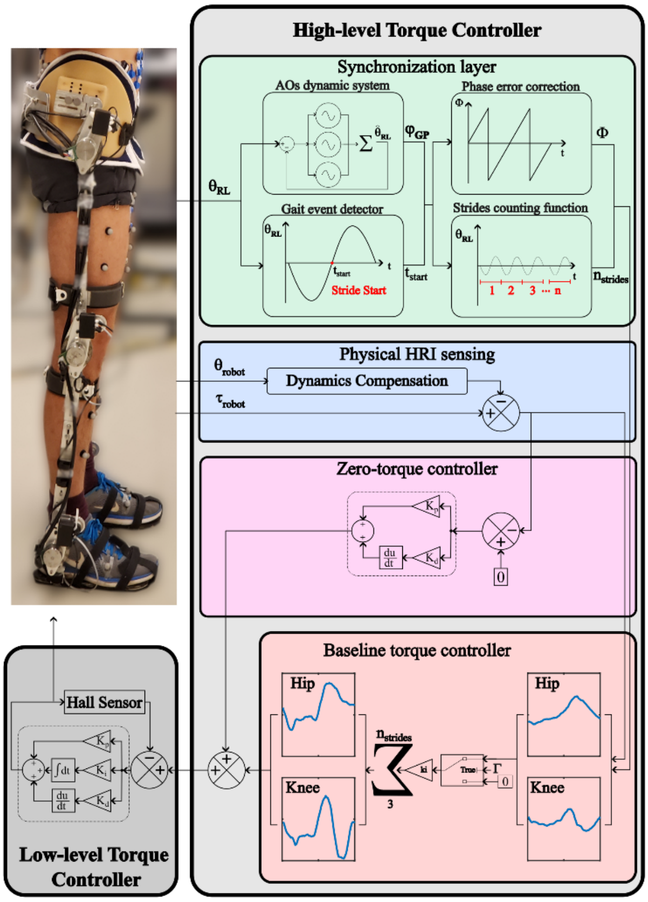

Fig. 2. Adaptive-Oscillators based transparent control. The controller consists in a high-level torque controller designed with a synchronization layer (green), physical human-robot sensing (blue) and a baseline torque controller (red), which runs in parallel to a zero-torque controller (pink); and a low-level torque controller, based on the electrical current of the motors.

The beginning of each gait cycle is identified by a gait event detection function, as indicated in Fig. 2. When $\theta_{RL}(t) \geq 0$ and $\theta_{RL}(t-1) < 0$ and the time of detection is greater than 70% of the last gait cycle, it is considered a real start cycle (t_{start}).

The phase $\varphi_{GP}(t)$ is corrected using a phase error function that relies on the start cycle time as follows:

$$\dot{\varphi_e}(t) = C_e \omega(t) e^{-\omega(t)(t-t_{start})} \tag{7}$$

$$C_e = k_e\big(P_e(t_{start}) - \varphi_e(t_{start})\big) \tag{8}$$

$$P_e(t_{start}) = \begin{cases} -\varphi_{GP}(t_{str}),\ if\ 0 \leq \varphi_{GP}(t_{str}) < \pi \\ 2\pi - \varphi_{GP}(t_{str}),\ if\ \pi \leq \varphi_{GP}(t_{str}) < 2\pi \end{cases} \tag{9}$$

where C_e is a proportional gain to determine the error at t_{start}, with a constant gain $k_e = 1$, and $P_e(t_{start})$ is the difference between the desired gait event and $\varphi_{GP}(t)$.

Then, the gait phase $\phi(t)$ of the system is calculated as follows:

$$\phi(t) = mod(\varphi_{GP}(t) + \varphi_e(t), 2\pi) \tag{10}$$

Since the AO dynamic system takes time to minimize $F(t)$ and synchronize the angle estimation when the system starts, the counting stride function is used to reject the first 2 strides.

2) *Physical human-robot interaction sensing*

Interaction torques between the ExoRoboWalker and the user are measured with a torque sensor attached to each joint (Fig. 1). To avoid the effects of the exoskeleton's dynamics on the measured torques, the inertial, Coriolis, centrifugal and gravitational forces should be properly canceled. The double-pendulum dynamic system is a common approach used to compute dynamic contributions of lower-limb exoskeletons [3][9][10]. Accordingly, the robot's equation of motion (11) and the net user-robot interaction (12) can be expressed as:

$$\tau_{dyn} = M(\theta)\ddot{\theta} + C(\theta, \dot{\theta})\dot{\theta} + G(\theta) \tag{11}$$

$$\tau_{UR}(t) = \tau_{sensor}(t) - \tau_{dyn}(t) \tag{12}$$

where τ_{dyn} is the required torque to move the joints, θ is the vector of relative angles of the links, M is the mass matrix, C is the Coriolis and centrifugal matrix, G is the gravitational matrix of the robot, $\tau_{UR}(t)$ is the physical interaction torque between user and exoskeleton at each joint, and $\tau_{sensor}(t)$ is the torque measured at each joint.

3) *Baseline torque controller*

The baseline torque controller generates a continuous output torque for the entire gait cycle based on the physical user-robot interaction (τ_{UR}) of the previous gait cycles as follows:

$$\tau_{BL}^{N} = \begin{cases} if\ \Gamma = True:\ \sum_{3}^{N=n_{str}} k_i \tau_{UR}^{N} \\ \quad if\ \Gamma = False:\ \tau_{BL}^{N-1} \end{cases} \tag{13}$$

$$\tau_{BL}^{N}(t) = spline(\tau_{BL}^{N}, \phi(t) + \varphi_{act}) \tag{14}$$

where Γ is a Boolean variable that indicates the beginning of a new gait cycle, identified by a gait event detection function embedded in the synchronization layer, N is the stride number, k_i is a convergence constant set as $k_i = 0.05$ for initial experiments, and φ_{act} is the phase of the actuator (low-level controller).

4) *Zero-torque controller*

The zero-torque controller is a small gain PD controller (TABLE I.) used to allow some volitional control of the exoskeleton by the user. Although the baseline torque controller imposes a torque profile to the next gait cycle to minimize the physical interaction with the user, some volitional control of the lower limbs is desirable to improve balance. Moreover, during the first steps, no compensation is applied to the actuators, and hence the exoskeleton has poor back-drivability [6][12]. The zero PD torque controller helps users to move their legs during the first gait cycles.

TABLE I. ZERO-TORQUE CONTROLLER GAINS

Gain	*Hip*	*Knee*	*Ankle*
k_p	1.0	1.0	0.5
k_d	0.05	0.05	0.05

C. Experimental Protocol

Eight subjects (five males and three females, 28.9±4.6 years, 69.9±14.4 kg, 1.56±0.53 m) participated in the study. They were asked to walk on a treadmill at three different gait speeds (0.4, 0.6, and 0.8 m/s) with and without the exoskeleton using 1) the proposed AO-based transparent controller and 2) a transparent controller we previously developed [6][12]. Each trial consisted of 80 strides at 0.4 m/s, 10 strides with linear increasing gait speed from 0.4 to 0.6 m/s, 20 strides at 0.6 m/s, 10 with linear increasing gait speed from 0.6 to 0.8 m/s, 20 strides at 0.8 m/s, 10 strides with linear decreasing gait speed from 0.8 to 0.6 m/s, 20 strides at 0.6 m/s, 10 strides with linear decreasing gait speed from 0.6 to 0.4 m/s, and 20 strides at 0.4 m/s, totaling 200 strides per trial.

Angular data was gathered at 100 Hz using seven XSens IMU sensors placed on the subjects' legs (Movella, NV, USA). The user-robot interaction torque was recorded by the torque sensors at each joint using a 500 Hz sampling frequency. The signal was low pass filtered using an elliptic filter.

The experimental protocol was approved by the Spaulding Rehabilitation Hospital Institutional Review Board. Subjects signed an informed consent form prior to participating in the study. All study procedures were carried out in accordance with all relevant guidelines and regulations.

III. Results and Discussion

The output of the synchronization layer shown presented in Fig. 3. The blue lines represent the measured variables, whereas the orange lines represent the estimated variables. Fig. 3 (a) shows the measured and estimated difference between the right and left hip angle, $\theta_{RL}(t)$ and $\hat{\theta}_{RL}(t)$, respectively. The estimation error $F(t)$ (i.e., difference between $\theta_{RL}(t)$ and $\hat{\theta}_{RL}(t)$) drops as the number of strides increases. The difference between the measured and estimated gait phase angle, $\phi(t)$, shown in Fig. 3 (b), also decreases very rapidly. These results suggest that the parameters set for the AOs dynamic system enable synchronization with the exoskeleton movement in about 3 strides. Fig. 3 (c) shows the fundamental frequency, $\omega(t)$, throughout the experimental trial of 200 strides at different gait speeds. At the end of the data collection, small oscillations in $\omega(t)$ suggest potential instabilities.

To evaluate the transparency of the system, the average physical user-robot interaction (τ_{UR}) was computed as the RMS value averaged across the hip, knee, and ankle data for each gait cycle. The results are presented in Fig. 4, where the blue line and red lines show the results for the AO-based transparent controller and the zero-impedance controlled we previously developed [6][12], respectively. Because the AO-based controller starts with just the zero PD torque controller to reduce the physical interaction forces between the user and the exoskeleton, the user is required to display great efforts to move the system at the beginning of the data collection. On the other hand, the zero-impedance controller we previously developed, could follow the movements of the user with small τ_{UR}[12]. However, as the number of strides increases and the AO dynamic system synchronizes with the user's gait, the baseline torque controller becomes more active in reducing the physical interaction with the user. This effect can be observed between the first to the fifth stride, when the physical interaction data appears to reach a steady state plateau, that is lower than the former transparent controller. The transparency of both methods is greater for high gait speeds. As such, when data was collected at 0.8 m/s (stride 120 to 140), the physical interaction of the previously developed controller is 60% as much as the AO-based one. It is also interesting to note that, at the end of the data collection, the physical interaction is greater than at the beginning of the experiment for both controllers, even when considering the same gait speed. Moreover, the AO-based method displayed an increased mean and standard deviation of the physical interaction data, denoting a potential instability of the system.

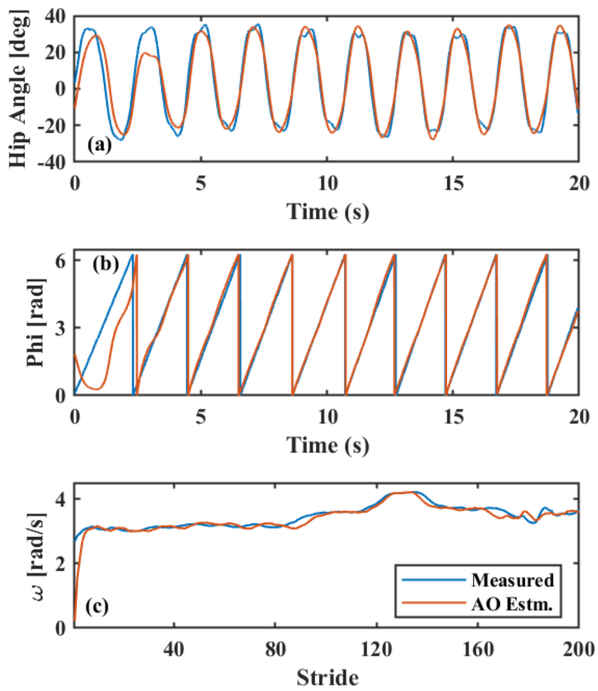

Fig. 3. Synchronization layer outputs. (a) Interlimb angle $\hat{\theta}_{RL}(t)$ and $\theta_{RL}(t)$, (b) corrected gait phase, $\phi(t)$, and (c) the fundamental frequency, $\omega(t)$.

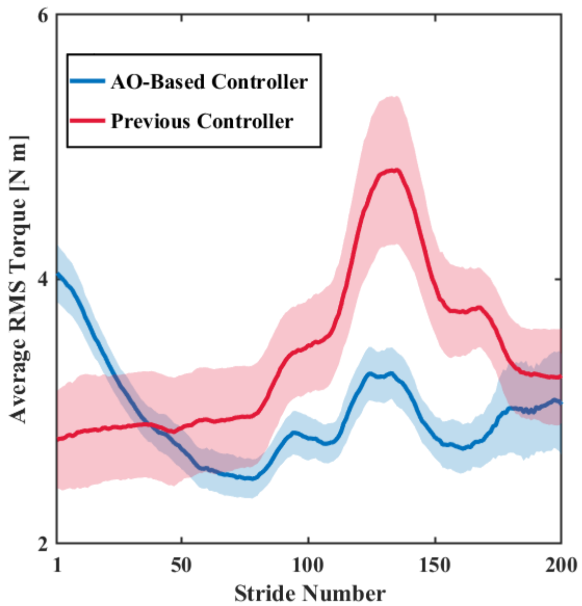

Fig. 4. Average RMS torque for each gait cycle computed as the average of the physical user-robot interaction at the hip, knee, and ankle joints. The solid lines are the average values. The shaded areas are the variability of the parameter computed as standard deviation.

IV. Conclusions

This paper presented a novel AOs-based torque controller for LLE designed to reduce the physical interaction between the user and the robot during gait. The proposed controller employs a synchronization layer that relies on a pool of AOs to estimate the gait phase and the start time of each gait cycle. The outputs of the sync layer are used by the baseline torque controller to generate a torque profile based on the user-robot physical interaction during previous strides. A zero-torque controller was utilized in parallel to the main controller to improve volitional control of the system by the user. Eight health subjects were tested at different gait speeds using the proposed controller as well as with a previously implemented transparent controller based on a zero-impedance model. The results showed significant improvements in the system's transparency, mainly at high gait speeds. Future work will seek to fine-tune the controller's parameters to further improve its stability and transparency.

Acknowledgment

This work was supported in part by the by grants from FAPES (Fundação de Amparo à Pesquisa e Inovação do Espírito Santo, TO: 946/2023, No. 2023-F0GWQ, TO: 565/2023, No.2023-BQK22), FINEP (Financiadora de Estudos e Projetos com recursos do FNDCT ref 2784/20), Brazilian National Council for Scientific and Technological Development (CNPq) project 402317/2023-8 and project 442445/2023-7, CAPES (Coordenação de Aperfeiçoamento de Pessoal de Nível Superior, finance Code 001).

References

[1] D. Pinto-Fernandez *et al.*, "Performance Evaluation of Lower Limb Exoskeletons: A Systematic Review," *IEEE Transactions on Neural Systems and Rehabilitation Engineering*, vol. 28, no. 7, pp. 1573–1583, Jul. 2020, doi: 10.1109/TNSRE.2020.2989481.

[2] R. Baud, A. R. Manzoori, A. Ijspeert, and M. Bouri, "Review of control strategies for lower-limb exoskeletons to assist gait," J NeuroEngineering Rehabil, vol. 18, no. 1, p. 119, Jul. 2021, doi: 10.1186/s12984-021-00906-3.

[3] R. M. Andrade and P. Bonato, "The Role Played by Mass, Friction, and Inertia on the Driving Torques of Lower-Limb Gait Training Exoskeletons," IEEE Transactions on Medical Robotics and Bionics, vol. 3, no. 1, pp. 125–136, Feb. 2021, doi: 10.1109/TMRB.2021.3052014.

[4] R. Yamamoto, S. Sasaki, W. Kuwahara, M. Kawakami, and F. Kaneko, "Effect of exoskeleton-assisted Body Weight-Supported Treadmill Training on gait function for patients with chronic stroke: a scoping review," J NeuroEngineering Rehabil, vol. 19, no. 1, p. 143, Dec. 2022, doi: 10.1186/s12984-022-01111-6.

[5] C. M. Diot, R. L. Thomas, L. Raess, J. G. Wrightson, and E. G. Condliffe, "Robotic lower extremity exoskeleton use in a non-ambulatory child with cerebral palsy: a case study," Disability and Rehabilitation: Assistive Technology, vol. 18, no. 5, pp. 497–501, Jul. 2023, doi: 10.1080/17483107.2021.1878296.

[6] R. M. Andrade, S. Sapienza, A. Mohebbi, E. E. Fabara, and P. Bonato, "Overground Walking With a Transparent Exoskeleton Shows Changes in Spatiotemporal Gait Parameters," IEEE Journal of Translational Engineering in Health and Medicine, vol. 12, pp. 182–193, 2024, doi: 10.1109/JTEHM.2023.3323381.

[7] S. M. Campbell, C. P. Diduch, and J. W. Sensinger, "Autonomous Assistance-as-Needed Control of a Lower Limb Exoskeleton With Guaranteed Stability," IEEE Access, vol. 8, pp. 51168–51178, 2020, doi: 10.1109/ACCESS.2020.2973373.

[8] R. M. Andrade, S. Sapienza, E. E. Fabara, and P. Bonato, "Trajectory Tracking Impedance Controller in 6-DoF Lower-Limb Exoskeleton for Over-Ground Walking Training: Preliminary Results," in 2021 International Symposium on Medical Robotics (ISMR), Nov. 2021, pp. 1–6. doi: 10.1109/ISMR48346.2021.9661558.

[9] R. Mendoza-Crespo, R. Soto, and J. L. Pons, "Transparent Mode for Lower Limb Exoskeleton," in Wearable Robotics: Challenges and Trends, J. González-Vargas, J. Ibáñez, J. L. Contreras-Vidal, H. van der Kooij, and J. L. Pons, Eds., Cham: Springer International Publishing, 2017, pp. 421–425. doi: 10.1007/978-3-319-46532-6_69.

[10] R. M. Andrade, S. Sapienza, and P. Bonato, "Development of a 'transparent operation mode' for a lower-limb exoskeleton designed for children with cerebral palsy," in 2019 IEEE 16th International Conference on Rehabilitation Robotics (ICORR), Jun. 2019, pp. 512–517. doi: 10.1109/ICORR.2019.8779432.

[11] D. Zanotto, T. Lenzi, P. Stegall, and S. K. Agrawal, "Improving transparency of powered exoskeletons using force/torque sensors on the supporting cuffs," in 2013 IEEE 13th International Conference on Rehabilitation Robotics (ICORR), Jun. 2013, pp. 1–6. doi: 10.1109/ICORR.2013.6650404.

[12] R. M. Andrade, S. Sapienza, A. Mohebbi, E. E. Fabara, and P. Bonato, "Experimental Evaluation of a Transparent Operation Mode for a Lower-Limb Exoskeleton Designed for Children with Cerebral Palsy," in 2023 IEEE/RSJ International Conference on Intelligent Robots and Systems (IROS), Oct. 2023, pp. 6062–6067. doi: 10.1109/IROS55552.2023.10342182.

[13] E. B. Küçüktabak et al., "Haptic Transparency and Interaction Force Control for a Lower Limb Exoskeleton," IEEE Transactions on Robotics, vol. 40, pp. 1842–1859, 2024, doi: 10.1109/TRO.2024.3359541.

[14] C. Camardella, F. Porcini, A. Filippeschi, S. Marcheschi, M. Solazzi, and A. Frisoli, "Gait Phases Blended Control for Enhancing Transparency on Lower-Limb Exoskeletons," IEEE Robotics and Automation Letters, vol. 6, no. 3, pp. 5453–5460, Jul. 2021, doi: 10.1109/LRA.2021.3075368.

[15] L. Righetti, J. Buchli, and A. J. Ijspeert, "Dynamic Hebbian learning in adaptive frequency oscillators," Physica D: Nonlinear Phenomena, vol. 216, no. 2, pp. 269–281, Apr. 2006, doi: 10.1016/j.physd.2006.02.009.

[16] E. Tricomi et al., "Underactuated Soft Hip Exosuit Based on Adaptive Oscillators to Assist Human Locomotion," IEEE Robotics and Automation Letters, vol. 7, no. 2, pp. 936–943, Apr. 2022, doi: 10.1109/LRA.2021.3136240.

[17] T. Yan, A. Parri, V. Ruiz Garate, M. Cempini, R. Ronsse, and N. Vitiello, "An oscillator-based smooth real-time estimate of gait phase for wearable robotics," Auton Robot, vol. 41, no. 3, pp. 759–774, Mar. 2017, doi: 10.1007/s10514-016-9566-0.

This work was supported in part by the by grants from FAPES (Fundação de Amparo à Pesquisa e Inovação do Espírito Santo, TO: 946/2023, No. 2023-F0GWQ, TO: 565/2023, No.2023-BQK22), FINEP (Financiadora de Estudos e Projetos com recursos do FNDCT ref 2784/20), Brazilian National Council for Scientific and Technological Development (CNPq) project 402317/2023-8 and project 442445/2023-7, CAPES (Coordenação de Aperfeiçoamento de Pessoal de Nível Superior, finance Code 001).